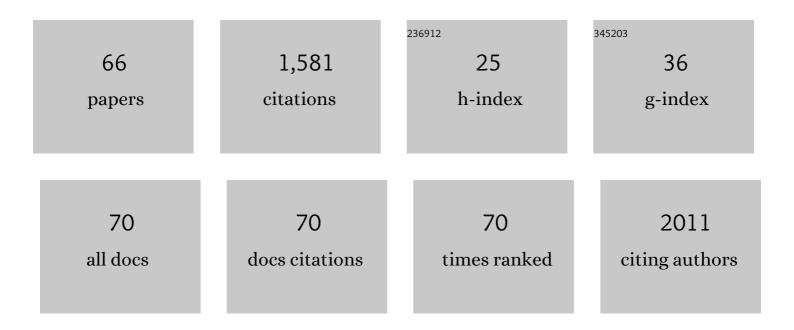
Francesco Iacoviello

List of Publications by Year in descending order

Source: https://exaly.com/author-pdf/8887180/publications.pdf Version: 2024-02-01



| # | Article | IF | CITATIONS |
|----|---|------|-----------|
| 1 | Antarctic ice sheet sensitivity to atmospheric CO ₂ variations in the early to mid-Miocene. Proceedings of the National Academy of Sciences of the United States of America, 2016, 113, 3453-3458. | 7.1 | 133 |
| 2 | Quantifying the anisotropy and tortuosity of permeable pathways in clay-rich mudstones using models based on X-ray tomography. Scientific Reports, 2017, 7, 14838. | 3.3 | 97 |
| 3 | Investigation of Hot Pressed Polymer Electrolyte Fuel Cell Assemblies via X-ray Computed Tomography. Electrochimica Acta, 2017, 242, 125-136. | 5.2 | 74 |
| 4 | Aqueous Inks of Pristine Graphene for 3D Printed Microsupercapacitors with High Capacitance. ACS Nano, 2021, 15, 15342-15353. | 14.6 | 60 |
| 5 | Laserâ€preparation of geometrically optimised samples for Xâ€ray nanoâ€CT. Journal of Microscopy, 2017, 267, 384-396. | 1.8 | 54 |
| 6 | The effect of non-uniform compression and flow-field arrangements on membrane electrode assemblies - X-ray computed tomography characterisation and effective parameter determination. Journal of Power Sources, 2019, 426, 97-110. | 7.8 | 46 |
| 7 | Novel laboratory investigation of huff-n-puff gas injection for shale oils under realistic reservoir conditions. Fuel, 2021, 284, 118950. | 6.4 | 43 |
| 8 | In situ compression and X-ray computed tomography of flow battery electrodes. Journal of Energy Chemistry, 2018, 27, 1353-1361. | 12.9 | 42 |
| 9 | Correlative study of microstructure and performance for porous transport layers in polymer electrolyte membrane water electrolysers by X-ray computed tomography and electrochemical characterization. International Journal of Hydrogen Energy, 2019, 44, 19519-19532. | 7.1 | 41 |
| 10 | Enhanced primary productivity and magnetotactic bacterial production in response to middle Eocene warming in the Neo-Tethys Ocean. Palaeogeography, Palaeoclimatology, Palaeoecology, 2014, 414, 32-45. | 2.3 | 37 |
| 11 | 4D nano-tomography of electrochemical energy devices using lab-based X-ray imaging. Nano Energy, 2018, 47, 556-565. | 16.0 | 37 |
| 12 | Virtual unrolling of spirally-wound lithium-ion cells for correlative degradation studies and predictive fault detection. Sustainable Energy and Fuels, 2019, 3, 2972-2976. | 4.9 | 37 |
| 13 | Enhanced composite plate impact damage detection and characterisation using X-Ray refraction and scattering contrast combined with ultrasonic imaging. Composites Part B: Engineering, 2020, 181, 107579. | 12.0 | 37 |
| 14 | A spinal organ of proprioception for integrated motor action feedback. Neuron, 2021, 109, 1188-1201.e7. | 8.1 | 36 |
| 15 | A Structure and Durability Comparison of Membrane Electrode Assembly Fabrication Methods: Self-Assembled Versus Hot-Pressed. Journal of the Electrochemical Society, 2018, 165, F3045-F3052. | 2.9 | 34 |
| 16 | X-ray tomography and modelling study on the mechanical behaviour and performance of metal foam flow-fields for polymer electrolyte fuel cells. International Journal of Hydrogen Energy, 2019, 44, 7583-7595. | 7.1 | 34 |
| 17 | Effect of Microstructure of Porous Transport Layer on Performance in Polymer Electrolyte Membrane Water Electrolyser. Energy Procedia, 2018, 151, 111-119. | 1.8 | 33 |
| 18 | Multiâ€Scale Imaging of Polymer Electrolyte Fuel Cells using Xâ€ray Micro―and Nanoâ€Computed Tomography, Transmission Electron Microscopy and Heliumâ€Ion Microscopy. Fuel Cells, 2019, 19, 35-42. | 2.4 | 31 |

| # | Article | IF | CITATIONS |
|----|--|------|-----------|
| 19 | 3D Imaging of Lithium Protrusions in Solidâ€State Lithium Batteries using Xâ€Ray Computed Tomography. Advanced Functional Materials, 2021, 31, 2007564. | 14.9 | 31 |
| 20 | Correlative acoustic time-of-flight spectroscopy and X-ray imaging to investigate gas-induced delamination in lithium-ion pouch cells during thermal runaway. Journal of Power Sources, 2020, 470, 228039. | 7.8 | 30 |
| 21 | Microstructure analysis and image-based modelling of face masks for COVID-19 virus protection. Communications Materials, 2021, 2, . | 6.9 | 30 |
| 22 | Provenance and geological significance of red mud and other clastic sediments of the Mugnano cave (Montagnola Senese, Italy). International Journal of Speleology, 2012, 41, 317-328. | 1.0 | 29 |
| 23 | MicroCT optimisation for imaging fascicular anatomy in peripheral nerves. Journal of Neuroscience Methods, 2020, 338, 108652. | 2.5 | 29 |
| 24 | X-ray Phase-Contrast Radiography and Tomography with a Multiaperture Analyzer. Physical Review Letters, 2017, 118, 243902. | 7.8 | 27 |
| 25 | Environmental magnetic implications of magnetofossil occurrence during the Middle Eocene Climatic Optimum (MECO) in pelagic sediments from the equatorial Indian Ocean. Palaeogeography, Palaeoclimatology, Palaeoecology, 2016, 441, 212-222. | 2.3 | 26 |
| 26 | Threeâ€Phase Segmentation of Solid Oxide Fuel Cell Anode Materials Using Lab Based Xâ€ray Nano omputed Tomography. Fuel Cells, 2017, 17, 75-82. | 2.4 | 26 |
| 27 | Imaging fascicular organization of rat sciatic nerves with fast neural electrical impedance tomography. Nature Communications, 2020, 11, 6241. | 12.8 | 24 |
| 28 | Metabolically diverse primordial microbial communities in Earth's oldest seafloor-hydrothermal jasper. Science Advances, 2022, 8, eabm2296. | 10.3 | 24 |
| 29 | The Imaging Resolution and Knudsen Effect on the Mass Transport of Shale Gas Assisted by Multi-length Scale X-Ray Computed Tomography. Scientific Reports, 2019, 9, 19465. | 3.3 | 22 |
| 30 | Prevention of lithium-ion battery thermal runaway using polymer-substrate current collectors. Cell Reports Physical Science, 2021, 2, 100360. | 5.6 | 22 |
| 31 | Pore structure development during hydration of tricalcium silicate by X-ray nano-imaging in three dimensions. Construction and Building Materials, 2019, 200, 318-323. | 7.2 | 21 |
| 32 | Three-Dimensional Visualization of Conductive Domains in Battery Electrodes with Contrast-Enhancing Nanoparticles. ACS Applied Energy Materials, 2018, 1, 4479-4484. | 5.1 | 20 |
| 33 | Evolution with depth from detrital to authigenic smectites in sediments from AND-2A drill core (McMurdo Sound, Antarctica). Clay Minerals, 2012, 47, 481-498. | 0.6 | 19 |
| 34 | Geosources for ceramic production: The clays from the Neogene–Quaternary Albegna Basin (southern Tuscany). Applied Clay Science, 2014, 91-92, 105-116. | 5.2 | 17 |
| 35 | In-situ X-ray tomographic imaging study of gas and structural evolution in a commercial Li-ion pouch cell. Journal of Power Sources, 2022, 520, 230818. | 7.8 | 17 |
| 36 | The multiscale hierarchical structure of Heloderma suspectum osteoderms and their mechanical properties. Acta Biomaterialia, 2020, 107, 194-203. | 8.3 | 16 |

| # | Article | IF | CITATIONS |
|----|---|------|-----------|
| 37 | Examining the effect of the secondary flow-field on polymer electrolyte fuel cells using X-ray computed radiography and computational modelling. International Journal of Hydrogen Energy, 2019, 44, 1139-1150. | 7.1 | 15 |
| 38 | Dendritic silver self-assembly in molten-carbonate membranes for efficient carbon dioxide capture. Energy and Environmental Science, 2020, 13, 1766-1775. | 30.8 | 15 |
| 39 | Correlation of X-ray diffraction signatures of breast tissue and their histopathological classification. Scientific Reports, 2017, 7, 12998. | 3.3 | 14 |
| 40 | Multimodal Phase-Based X-Ray Microtomography with Nonmicrofocal Laboratory Sources. Physical Review Applied, 2017, 8, . | 3.8 | 14 |
| 41 | Thermally Driven SOFC Degradation in 4D: Part I. Microscale. Journal of the Electrochemical Society, 2018, 165, F921-F931. | 2.9 | 14 |
| 42 | Xâ€ray Nanoâ€computed Tomography of Electrochemical Conversion in Lithiumâ€ion Battery. ChemSusChem, 2019, 12, 3550-3561. | 6.8 | 14 |
| 43 | Evidence of structural cavities in 3D printed acetabular cups for total hip arthroplasty. Journal of Biomedical Materials Research - Part B Applied Biomaterials, 2020, 108, 1779-1789. | 3.4 | 14 |
| 44 | Three dimensional characterisation of chromatography bead internal structure using X-ray computed tomography and focused ion beam microscopy. Journal of Chromatography A, 2018, 1566, 79-88. | 3.7 | 13 |
| 45 | Thermally Driven SOFC Degradation in 4D: Part II. Macroscale. Journal of the Electrochemical Society, 2018, 165, F932-F941. | 2.9 | 12 |
| 46 | Anomalous transport of colloids in heterogeneous porous media: A multi-scale statistical theory. Journal of Colloid and Interface Science, 2022, 617, 94-105. | 9.4 | 11 |
| 47 | A Multiscale Xâ€Ray Tomography Study of the Cycledâ€Induced Degradation in Magnesium–Sulfur Batteries. Small Methods, 2021, 5, e2001193. | 8.6 | 10 |
| 48 | Clay minerals in cave sediments and terra rossa soils in the Montagnola Senese karst massif (Italy). Geological Quarterly, 2013, 57, . | 0.2 | 10 |
| 49 | Miocene Glacial Dynamics Recorded by Variations in Magnetic Properties in the ANDRILLâ€2A Drill Core. Journal of Geophysical Research: Solid Earth, 2019, 124, 2297-2312. | 3.4 | 9 |
| 50 | Ultra high-resolution biomechanics suggest that substructures within insect mechanosensors decisively affect their sensitivity. Journal of the Royal Society Interface, 2022, 19, 20220102. | 3.4 | 9 |
| 51 | Improved X-ray computed tomography reconstruction of the largest fragment of the Antikythera Mechanism, an ancient Greek astronomical calculator. PLoS ONE, 2018, 13, e0207430. | 2.5 | 8 |
| 52 | Packed bed compression visualisation and flow simulation using an erosion-dilation approach. Journal of Chromatography A, 2020, 1611, 460601. | 3.7 | 7 |
| 53 | Microporous Biodegradable Films Promote Therapeutic Angiogenesis. Advanced Healthcare Materials, 2020, 9, e2000806. | 7.6 | 7 |
| 54 | Rapid Preparation of Geometrically Optimal Battery Electrode Samples for Nano Scale X-ray Characterisation. Journal of the Electrochemical Society, 2020, 167, 060512. | 2.9 | 7 |

FRANCESCO IACOVIELLO

| # | Article | IF | CITATIONS |
|----|---|-----|-----------|
| 55 | An open-source platform for 3D-printed redox flow battery test cells. Sustainable Energy and Fuels, 2022, 6, 1529-1540. | 4.9 | 7 |
| 56 | A multi-method assessment of 3D printed micromorphological osteological features. International Journal of Legal Medicine, 2022, 136, 1391-1406. | 2.2 | 6 |
| 57 | Evaluating microstructure evolution in an SOFC electrode using digital volume correlation. Sustainable Energy and Fuels, 2018, 2, 2625-2635. | 4.9 | 4 |
| 58 | Motion-enhancement assisted digital image correlation of lithium-ion batteries during lithiation. Journal of Power Sources, 2022, 527, 231150. | 7.8 | 4 |
| 59 | In situ x-ray computed tomography of zinc–air primary cells during discharge: correlating discharge rate to anode morphology. JPhys Materials, 2022, 5, 014001. | 4.2 | 4 |
| 60 | The Time-Dependent Role of Bisphosphonates on Atherosclerotic Plaque Calcification. Journal of Cardiovascular Development and Disease, 2022, 9, 168. | 1.6 | 3 |
| 61 | Alteration of volcanic deposits in the ANDRILL AND-1B core: Influence of paleodeposition, eruptive style, and magmatic composition. , 2013, 9, 275-286. | | 2 |
| 62 | Early Miocene Antarctic glacial history: new insights from heavy mineral analysis from ANDRILL AND-2A drill core sediments. International Journal of Earth Sciences, 2015, 104, 853-872. | 1.8 | 2 |
| 63 | High-resolution imaging of depth filter structures using X-ray computed tomography. Journal of Materials Science, 2021, 56, 15313. | 3.7 | 1 |
| 64 | Liposome Sterile Filtration Characterization via X-ray Computed Tomography and Confocal Microscopy. Membranes, 2021, 11, 905. | 3.0 | 1 |
| 65 | Fascicular Organisation and Neuroanatomy of the Porcine and Human Vagus Nerves: Allowing for Spatially Selective Vagus Nerve Stimulation. FASEB Journal, 2022, 36, . | 0.5 | 1 |
| 66 | Use of Photon Scattering Interactions in Diagnosis and Treatment of Disease. , 2018, , 135-158. | | 0 |